

Preparation of Electrode of Copper-Nickel Composite Material and Its Capacitance Performance

Xiuxia Zhang^{1,2*}, Chaohui Li¹, Qianyu Ji¹

¹School of Electrical and Information Engineering, Beifang University of Nationalities, Yinchuan, China

²Optoelectronic Information Engineering, Hefei University of Technology, Hefei, China

Email: *xxuazh@126.com

How to cite this paper: Zhang, X.X., Li, C.H. and Ji, Q.Y. (2016) Preparation of Electrode of Copper-Nickel Composite Material and Its Capacitance Performance. *World Journal of Nano Science and Engineering*, 6, 165-176.

<http://dx.doi.org/10.4236/wjnse.2016.64015>

Received: October 14, 2016

Accepted: December 20, 2016

Published: December 23, 2016

Copyright © 2016 by authors and Scientific Research Publishing Inc. This work is licensed under the Creative Commons Attribution International License (CC BY 4.0).

<http://creativecommons.org/licenses/by/4.0/>



Open Access

Abstract

Nickel oxide/copper oxide composites are prepared. Then the composites were transferred into autoclave and thermal sinter under different temperature and different time. As-prepared composites were analyzed by XRD, and it was concluded that with the increase of hydrothermal time, content of NiO and Ni_{0.75}Cu_{0.25}O increases, but particles become smaller; it would improve the electrochemical activity. By SEM images directed lower crystallinity of composites, deeper porosity and rougher surface would have better electrochemical activity. The electrochemical performance was investigated by cyclic voltametry, AC impedance and galvanostatic charge-discharge. All results show that under the condition of 150°C 30 h, the electrochemical performance is the best. The specific capacitance was 225.67 F·g⁻¹ at the charge-discharge current of 1 A·g⁻¹.

Keywords

Hydrothermal Method, Nickel Oxide, Copper Oxide, Composites, Capacitance

1. Introduction

Supercapacitor has higher power density compared with better battery, and has higher specific capacity and energy density compared with better conventional capacitor [1] [2], and mainly used in aerospace, computers, electric toys and other fields [3] [4]. Carbon materials, metal oxides and their composites, conductive polymers and other materials were used in ultracapacitors [5] [6] [7] [8]. Meng prepared graphite oxide by Hummers, then synthesis grapheme-zinc oxide by solvothermal method; the specific capacity was only 9 F·g⁻¹ at a current density of 1·g⁻¹ [9]. Using RuO₂ in ultracapaci-

tors, specific capacitance could reach 551 F/g. But the very expensive costs of RuO₂ would limit its application and development. So, science researcher must seek low cost metal oxides. Now, MnO₂, NiO and CuO Metal oxide composites were used in making ultracapacitors [7]-[12].

In this paper, copper-nickel oxide was successfully prepared by hydrothermal method. In 6 mol/L KOH electrolyte, the specific capacitance was 225.67 F·g⁻¹ at the charge-discharge current of 1 A·g⁻¹ and induced charge transfer resistance (R_{ct}) and diffusion impedance (Warburg impedance) [10] [11] were relatively low.

2. Experiment

2.1. Preparation of Electrode

The amount of 0.5 mol/L CuCl₂ solution 5 mL and 0.5 mol/L NiCl₂ solution 15 mL mixed in a beaker, then, weigh 1 mol/L NaOH solution 20 mL, at 60°C water bath magnetic stirring the pot, titration 40 minutes, then transferred to the reaction vessel, the degree of filling is 80%. Under the condition of 150°C, respectively reflect 10 h, 20 h, 30 h. Under the condition of 135°C, 150°C, reflect 30 h. The hydrothermal sample with distilled water and absolute ethanol washed six times, 90°C in blast oven dried 6 hours, then the dried sample was placed in a muffle furnace 300°C calcined 3 h, finally obtained the active material. The preparation of the active substance, acetylene black (AB), polyvinylidene fluoride (PVDF), the mass ratio of 80:15:5 placed in a beaker, grinding evenly, then added N-methyl-2-pyrrolidone network (NWP), stir into a paste-like. Then the mixture was uniformly coated on a foamed nickel, a coating area of 1 × 1 cm², under the condition of 90°C, dried for 12 hours, weighed its quality. Subtracting the mass of the uncoated nickel foam, the quality of the active substance can be calculated. Finally, under the 10 Mpa pressure, the sample was tablet and placed in 6 mol/L KOH solution and soaked about 24 hours.

2.2. Performance Testing

The test device is a Shimadzu SHIMADZU's XRD-6000, test conditions: CuK α as a radiation source target, the tube voltage 30 kV, tube current 50 mA, scanning speed 4°/min, scanning range (2 θ) 10° - 80°. And used Shimadzu SHIMADZU's SSX-550 scanning electron microscope (SEM) to observe the sample surface morphology, observed speed is 5000 times. In this study, the electrochemical analysis test was used Shanghai Chen Hua companies producing CHI604B/630B electrochemical workstation by three-electrode system, the working electrode was an electrode active materials which had prepared, the counter electrode was a platinum electrode, the reference electrode was a saturated calomel electrode.

3. The Analysis of Experimental Data

3.1. The SEM Characterization

Figure 1 to **Figure 5** are the SEM images of NiO/CuO composites samples at different

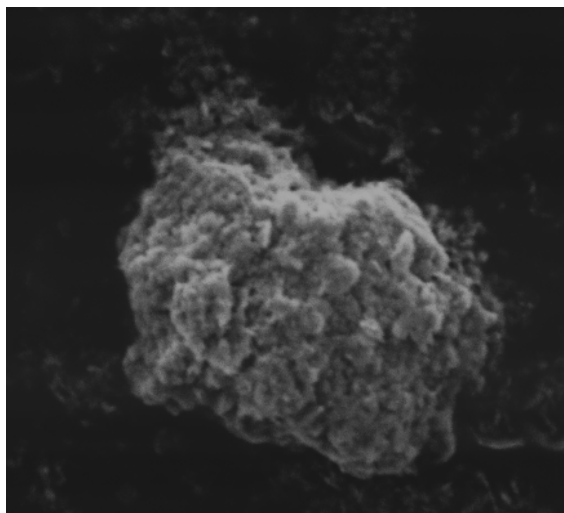


Figure 1. SEM image of NiO/CuO composites under 120°C 30 h.

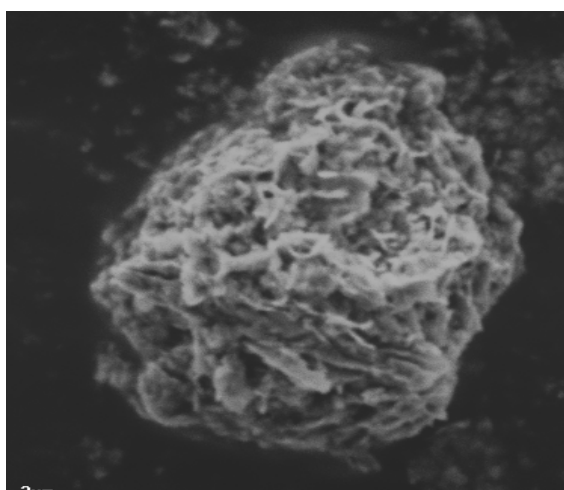


Figure 2. SEM image of NiO/CuO composites under 135°C 30 h.

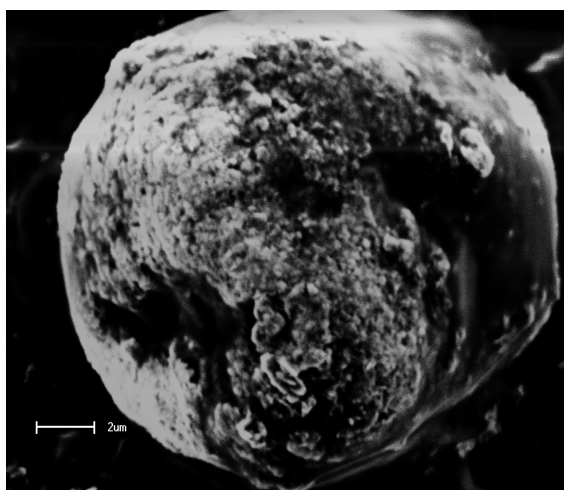


Figure 3. SEM image of NiO/CuO composites under 135°C 20 h.

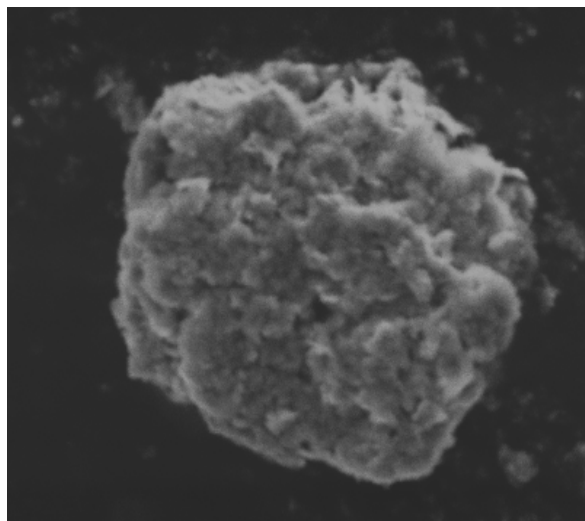


Figure 4. SEM image of NiO/CuO composites under 150°C 10 h.

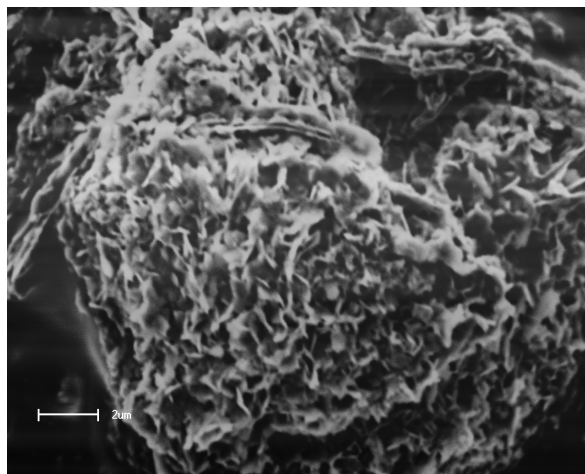


Figure 5. SEM image of NiO/CuO composites at 150°C 30 h.

hydrothermal conditions (5000 \times). As can be seen from the figures, the samples have different degrees of agglomeration. In **Figure 3**, the sample has poor electrochemical performance, because it with smooth surface and without pores and gully, that may affect the embedding and extraction of the electrolyte ion. The agglomeration of **Figure 3** is the most obvious among all figures. Compared to **Figure 3**, **Figure 1** and **Figure 4** have formed voids. The sample of **Figure 5** has a deeper porosity, rougher surface, a relatively low degree of crystallinity. So, it would conclude that the sample in **Figure 5** possess best capacitance performance among all samples.

3.2. The Analysis of XRD Phase

Figure 6 is XRD patterns of Copper-nickel composite at different hydrothermal time under 150°C, **Figure 7** is XRD patterns of Copper-nickel composite at different hydrothermal temperatures in 30 h.

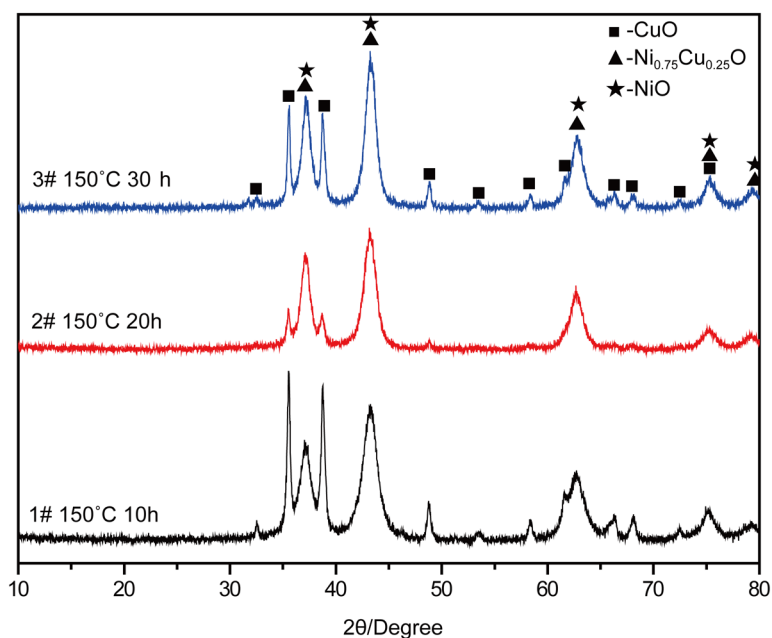


Figure 6. XRD patterns at different hydrothermal times under 150°C.

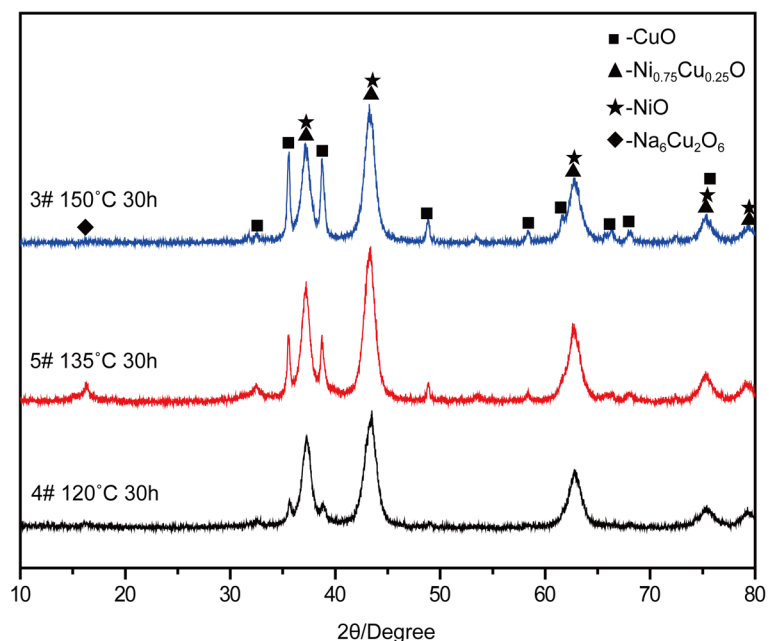


Figure 7. XRD patterns at different hydrothermal temperatures in 30 h.

Figure 7 appears $\text{Na}_6\text{Cu}_2\text{O}_6$, probably because the precipitation did not clean up. At diffraction angle 2θ of 37.248° , 43.286° , 62.852° , emerge diffraction peaks of NiO and $\text{Ni}_{0.75}\text{Cu}_{0.25}\text{O}$ and at 35.571° and 38.726° , as do CuO. At 150°C , with the increase of hydrothermal time the diffraction peaks of NiO and $\text{Ni}_{0.75}\text{Cu}_{0.25}\text{O}$ become more and more obvious, and the occurrence of the diffraction peak also width broadening, content of NiO and $\text{Ni}_{0.75}\text{Cu}_{0.25}\text{O}$ increase too and particles become smaller, the electrochemical

activity would improve [12]. From **Figure 7**, under the condition of same hydrothermal time (30 h), with the increase of hydrothermal temperature, the diffraction peaks of NiO and $\text{Ni}_{0.75}\text{Cu}_{0.25}\text{O}$ become more and more obvious, and the width of the peak broaden.

3.3. Cyclic Voltammetry

Cu:Ni = 1:3 30 h at different hydrothermal temperatures and different scanning rates from **Figure 8** to **Figure 10**, at the scanning rate of $50 \text{ mv}\cdot\text{s}^{-1}$, the edox peaks is not obvious, just sweep the reduction peak, the current is the largest. With the reduce of the scanning rates, the redox peak of the three samples become more obvious. The CV curves of Cu:Ni = 1:3 150°C at different hydrothermal times and different scanning rates. From **Figure 11** to **Figure 13**, with the decrease of scanning rate, redox peaks of three samples become more obvious, and at the hydrothermal condition of 150°C 30 h, have good electrochemical properties Equations.

3.4. AC Impedance

Figure 14, **Figure 15** are the AC impedances of Cu:Ni = 1:3 at different hydrothermal times and different hydrothermal temperatures.

AC impedance curve of the sample can be divided into two parts, the high-frequency and low-frequency region area. Intersection of curve and the real axis represent inner electrode impedance (equivalent to R_b), it concludes impedance of electrolyte ions, the intrinsic impedance of the electrode material and contact resistance of Electrically active material and the current collector. From **Figure 9** and **Figure 10**, intersection value of five samples and the Z' axis is very small, indicating that the internal impedance is small and almost the same. The semicircle of high frequency region represents induced

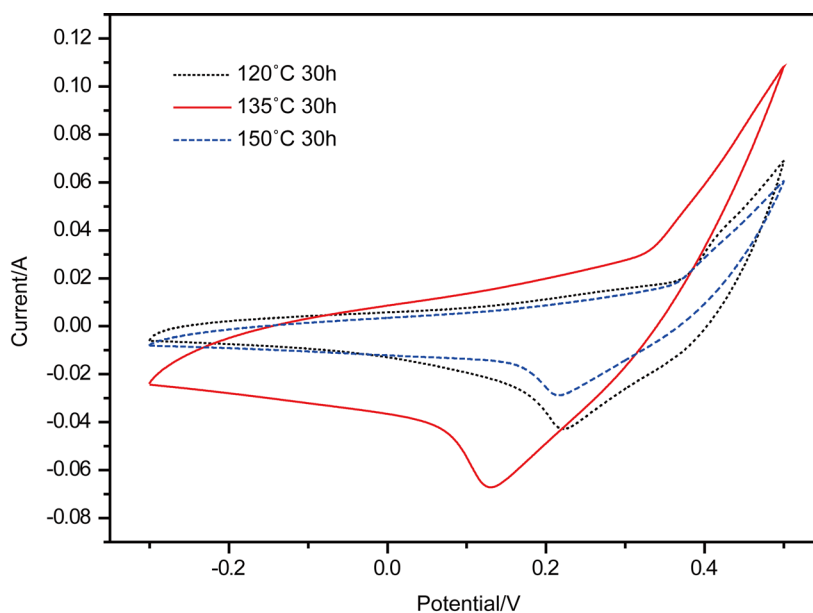


Figure 8. CV curves of $50 \text{ mv}\cdot\text{s}^{-1}$ scanning rates.

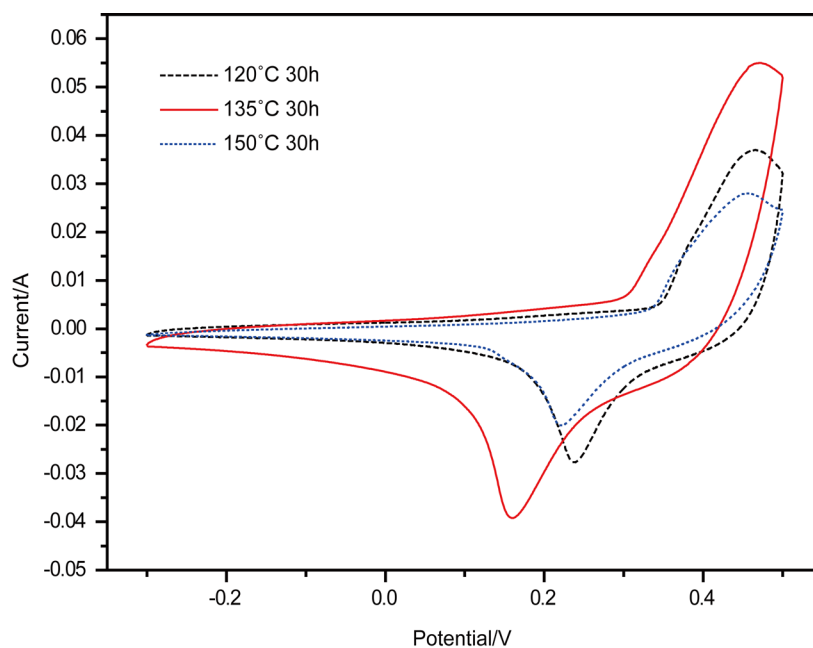


Figure 9. CV curves of $10 \text{ mv}\cdot\text{s}^{-1}$ scanning rates.

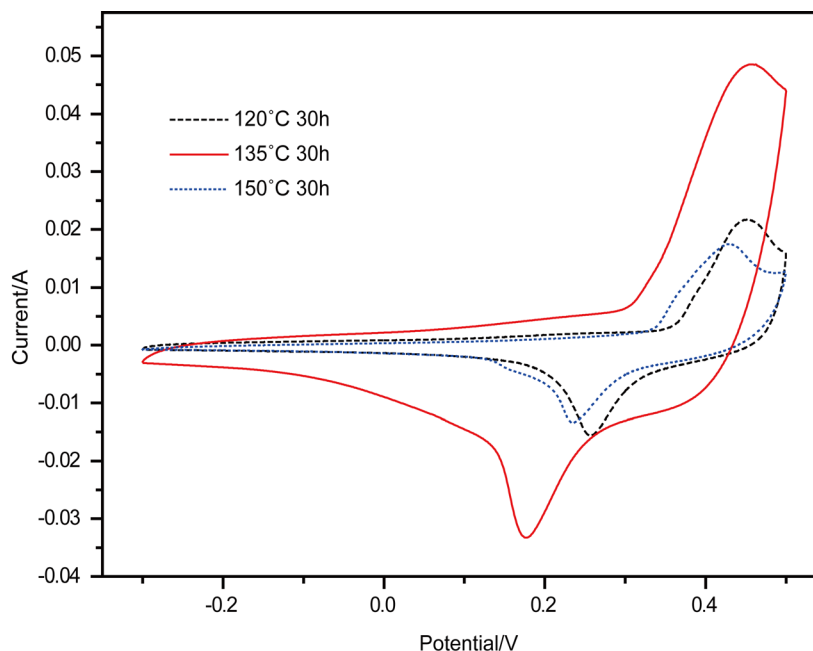


Figure 10. CV curves of $5 \text{ mv}\cdot\text{s}^{-1}$ scanning rates.

charge transfer resistance, frequency image in the embedded thumbnail in **Figure 13** and **Figure 14**. Under 150°C 30 h hydrothermal conditions, induced charge transfer resistance is the minimum. In low frequency region, slightly inclined straight line represents diffusion impedance (Warburg impedance). Impedance spectroscopy to achieve the desired behavior at low frequency capacitance line for line parallel to Z'' linear axis. So sample at 150°C 30 h hydrothermal conditions with minimal resistance.

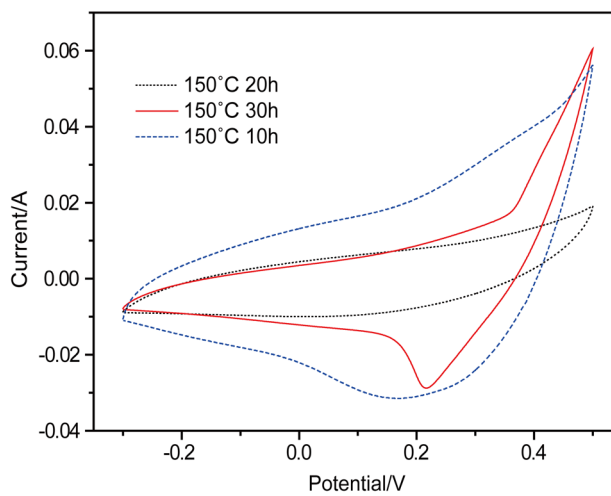


Figure 11. CV curves of 50 $\text{mV}\cdot\text{s}^{-1}$ scanning rates.

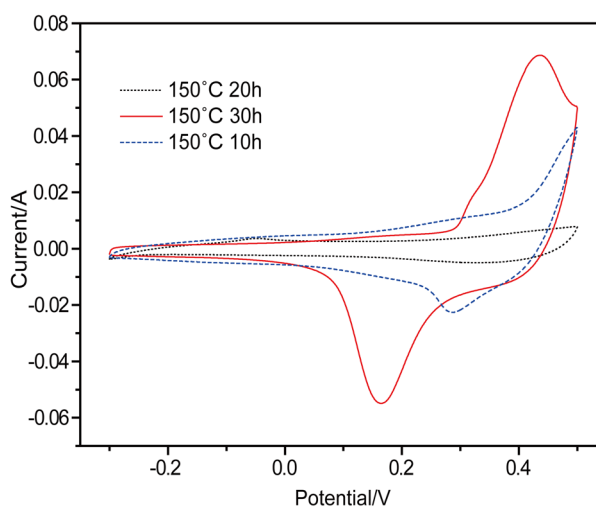


Figure 12. CV curves of 10 $\text{mV}\cdot\text{s}^{-1}$ scanning rates.

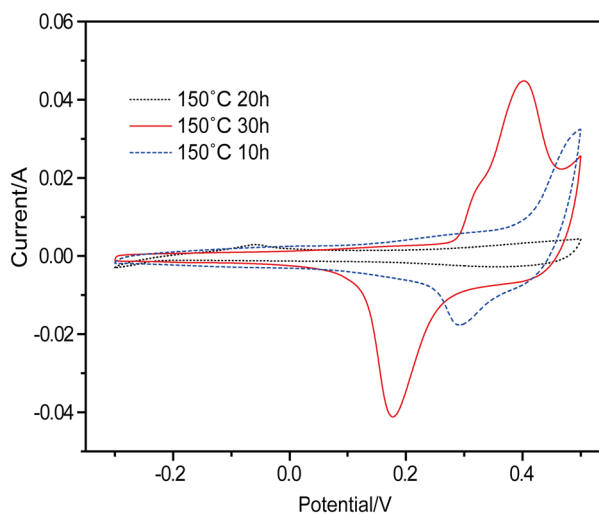


Figure 13. CV curves of 5 $\text{mV}\cdot\text{s}^{-1}$ scanning rates.

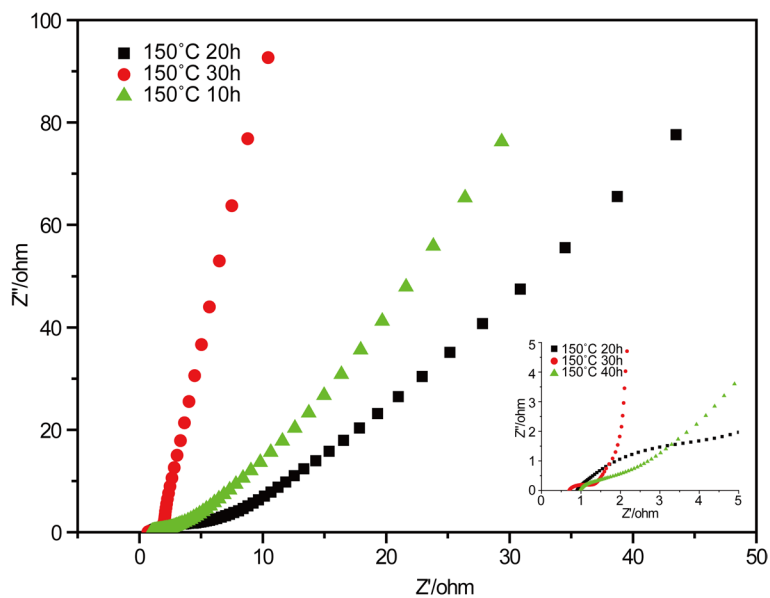


Figure 14. AC impedance of Cu:Ni = 1:3 150°C at different hydrothermal times.

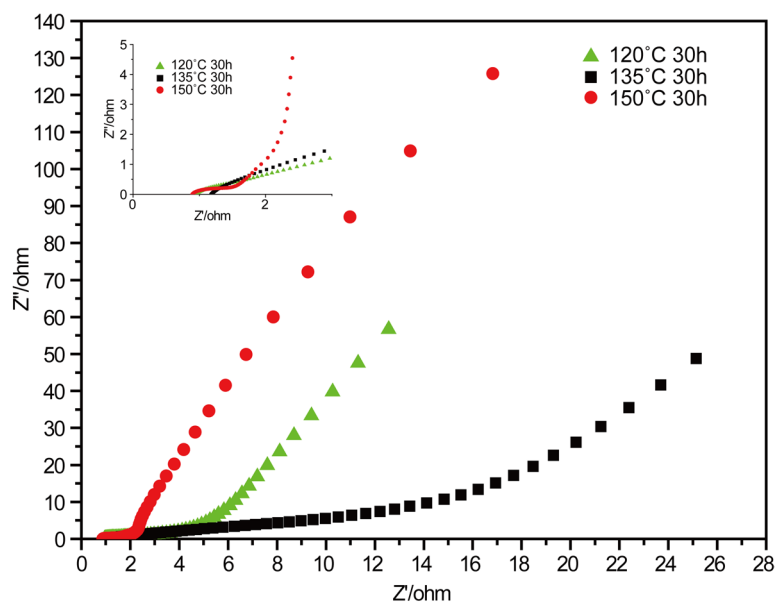


Figure 15. AC impedance of Cu:Ni = 1:3, 30 h at different hydrothermal temperatures.

3.5. Constant Current Charge and Discharge Characteristics

Figure 16 to **Figure 19** are the charge-discharge curves of Cu:Ni = 1:3 at different hydrothermal times and different hydrothermal temperatures. From **Figure 16** and **Figure 17**, at the 135°C has longest charging and discharging time. In 1 A·g⁻¹ current density, three sets of samples of the discharge duration will remain at 100 s, while at 135°C has maximum charging time. Compared to the condition of 1 A·g⁻¹ current density, discharge time of 0.5 A·g⁻¹ current density is the twice. And under the condition of 135°C 30 h, charge and discharge time is still the longest.

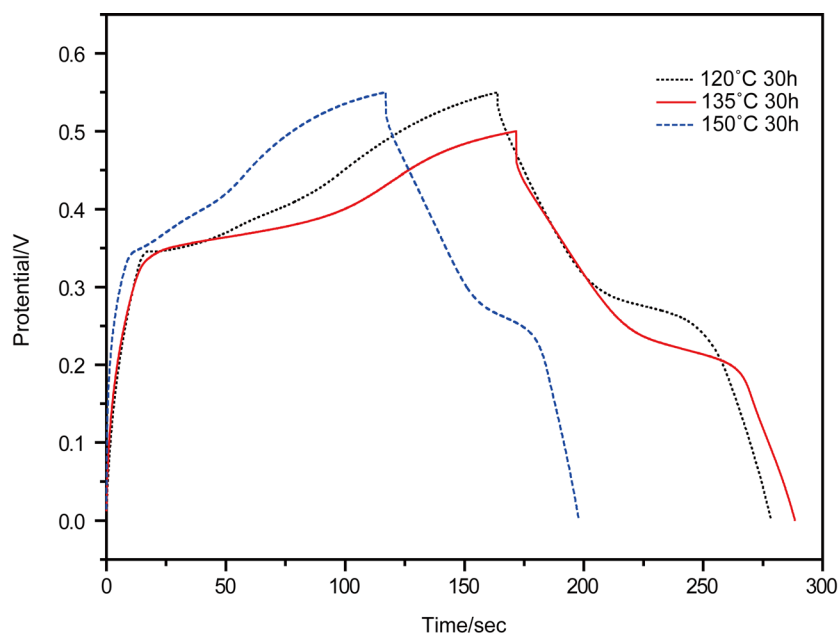


Figure 16. Charge-discharge curves of Cu:Ni = 1:3 30 h at different hydrothermal temperatures in $1 \text{ A}\cdot\text{g}^{-1}$.

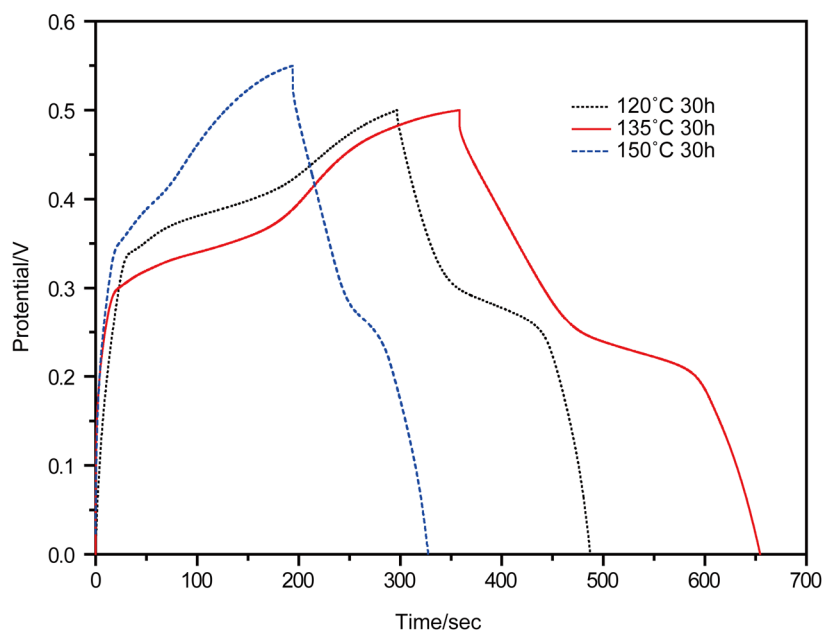


Figure 17. Charge-discharge curves of Cu:Ni = 1:3 30 h at different hydrothermal temperatures in $0.5 \text{ A}\cdot\text{g}^{-1}$.

From **Figure 18**, at $1 \text{ A}\cdot\text{g}^{-1}$ current density, under the hydrothermal condition of 150°C 30 h, the charge and discharge time is the longest. At $0.5 \text{ A}\cdot\text{g}^{-1}$ current density, under the hydrothermal condition of 150°C 10 h, the charge and discharge time is the longest, and under the hydrothermal condition of 150°C 20 h, has the maximum charge-discharge voltage, and it can reach 0.55 V.

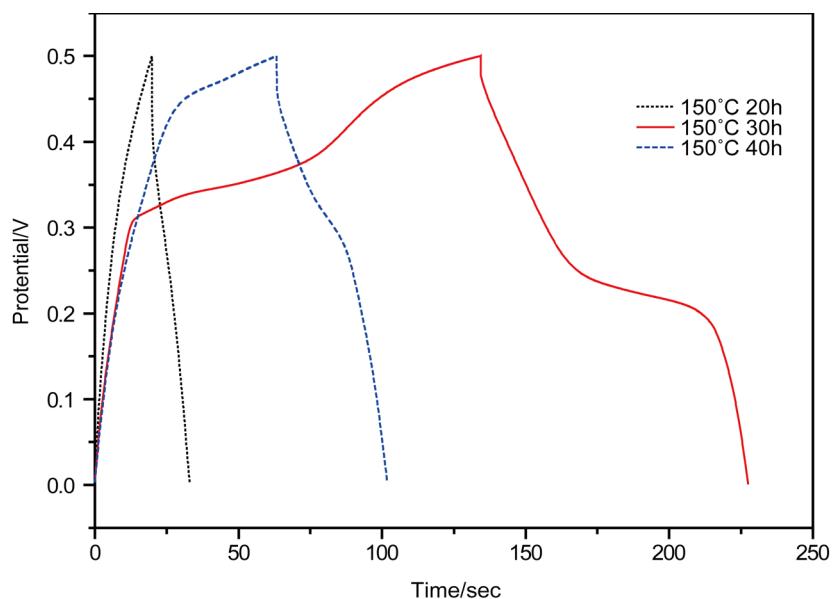


Figure 18. Charge-discharge curves of Cu:Ni = 1:3 30 h at different hydrothermal times in 1 A·g⁻¹.

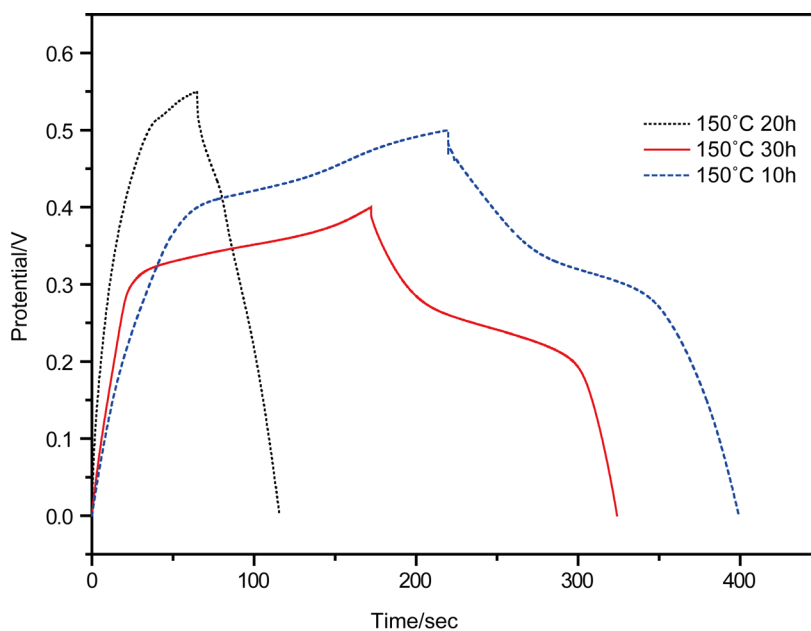


Figure 19. Charge-discharge curves of Cu:Ni = 1:3 30 h at different hydrothermal times in 0.5 A·g⁻¹.

4. Summary

In the experiment, we successfully made nickel oxide and copper oxide composites by hydrothermal synthesis. By comparing 150°C under different hydrothermal time and 30 h under different hydrothermal temperature, to find different electrochemical properties, it was found that after 150°C 30 h, hydrothermal reaction sample has the best electrochemical performance. Under the condition of 150°C 30 h, CV curve redox

peaks are obvious; charge and discharge time is the longest. The specific capacitance was $225.67 \text{ F}\cdot\text{g}^{-1}$ at the charge-discharge current of $1 \text{ A}\cdot\text{g}^{-1}$. Different hydrothermal time, hydrothermal temperature and heating rate are very important for the growth of sample particle morphology

Acknowledgements

The project was supported by the National Natural Science Foundation of China (51365001).

References

- [1] Conway, B.E. (1991) Transition from “Supercapacitor” to “Battery” Behavior in Electrochemical Energy Storage. *Journal of the Electrochemical Society*, **138**, 1539-1548. <https://doi.org/10.1149/1.2085829>
- [2] Futaba, D.N., Hata, K., Yamada, T., Hiraoka, T., Hayamizu, Y., Kakudate, Y., Tanaike, O., Hatori, H., Yumura, M. and Iijima, S. (2006) Shape-Engineerable and Highly Densely Packed Single-Walled Carbon Nanotubes and Their Application as Super-Capacitor Electrodes. *Nature Materials*, **5**, 987-994. <https://doi.org/10.1038/nmat1782>
- [3] Faggiolo, E., Rena, P., Danel, V. and Andrieuc, X. (1999) Supercapacitors for the Energy Management of Electric Vehicles. *J. Power Sources*, **84**, 261-269. [https://doi.org/10.1016/S0378-7753\(99\)00326-2](https://doi.org/10.1016/S0378-7753(99)00326-2)
- [4] Zhang, Z.A. and Deng, M.G. (2003) Characteristics and Applications of Electrochemical Capacitors. *Electronic Components & Materials*, **22**, 1.
- [5] Zhang, B.L., Zhao, H., Zhang, X. and Qian, L.J. (2003) Application of Supercapacitor in Hybrid Electric Vehicle. *Automobile Research & Development*, **5**, 48.
- [6] Lam, L.T., Newnham, R.H., Ozgun, H. and Fleming, F.A. (2000) Advanced Design of Valve-Regulated Lead-Acid Battery for Hybrid Electric Vehicles. *Journal of Power Sources*, **88**, 92-97. [https://doi.org/10.1016/S0378-7753\(99\)00515-7](https://doi.org/10.1016/S0378-7753(99)00515-7)
- [7] Zhang, S.S., Xu, K. and Jow, T.R. (2004) Electrochemical Impedance Study on the Low Temperature of Li-Ion Batteries. *Electrochimica Acta*, **49**, 1057-1061. <https://doi.org/10.1016/j.electacta.2003.10.016>
- [8] Xu, M.W., Bao, S.J. and Li, H.L. (2007) Synthesis and Characterization of Mesoporous Nickel Oxide for Electrochemical Capacitor. *Journal of Solid State Electrochemistry*, **11**, 372-377. <https://doi.org/10.1007/s10008-006-0155-6>
- [9] Kiani, M.A., Mousavi, M.F. and Ghasemi, S. (2010) Size Effect Investigation on Battery Performance: Comparison between Micro- and Nano-Particles of $\beta\text{-Ni(OH)}_2$ as Nickel Battery Cathode Material. *Journal of Power Sources*, **195**, 5794-5800. <https://doi.org/10.1016/j.jpowsour.2010.03.080>
- [10] Wang, X.F. (2003) Preparation of Ultra-Fine Ruthenium Oxide as an Electrode Materials for Electrochemical Capacitors. *Chinese Journal of Inorganic Chemistry*, **19**, 371-375.
- [11] Cai, T., Zhu, P. and Ren, Z. (2014) Preparation and Performances of RuO_2 and Its Composite Electrodes. *Micronanoelectronic Technology*, **8**, 508-511.
- [12] Gujar, T.P., Shinde, V.R., Lokhande, C.D., *et al.* (2007) Spray Deposited Amorphous RuO_2 for an Effective Use in Electrochemical Supercapacitor. *Electrochemistry Communications*, **9**, 504-510. <https://doi.org/10.1016/j.elecom.2006.10.017>



Submit or recommend next manuscript to SCIRP and we will provide best service for you:

Accepting pre-submission inquiries through Email, Facebook, LinkedIn, Twitter, etc.

A wide selection of journals (inclusive of 9 subjects, more than 200 journals)

Providing 24-hour high-quality service

User-friendly online submission system

Fair and swift peer-review system

Efficient typesetting and proofreading procedure

Display of the result of downloads and visits, as well as the number of cited articles

Maximum dissemination of your research work

Submit your manuscript at: <http://papersubmission.scirp.org/>

Or contact wjnse@scirp.org